First ESAFORM Conference on Material Forming, Sophia Antipolis, France, 16–20 March 1998

Inhomogeneities in the stress and strain rate fields during Gleeble testing

Asbjørn Mo*, Ivar Farup*, and Jean-Marie Drezet#

* SINTEF Materials Technology,
P. O. Box 124 Blindern,
N-0314 Oslo, Norway

Laboratoire de métallurgie physique,
Ecole Polytechnique Fédérale de Lausanne, MX-G,
CH-1015, Lausanne, Switzerland

Abstract

By means of a Gleeble machine, the authors recently measured the flow stress at steady state creep in an AA3103 aluminium alloy for temperatures and strain rates relevant for thermally induced deformations in DC casting. The strain rate was determined by measuring the global radial strain rate at the specimen centre by an extensometer, and the stress was set equal to the force in the axial direction divided by the cross section area at the specimen centre. Such a method is based upon the assumption of a homogeneous distribution of stress and strain rate. However, Gleeble specimens are heated by the Joule effect leading to temperature gradients in the axial direction and the specimens are often non-cylindrical with a reduced diameter at the centre. This leads to inhomogeneities in the stress and strain rate fields which in the present paper are studied by finite element modelling. It is shown that the stress and strain rate inhomogeneities can be significant. It is furthermore pointed out that in spite of the inhomogeneities, the global radial strain rate and the axial force divided by the cross section area at the specimen centre can be relatively close to what the respective strain rate and stress values would have been if the conditions actually were homogeneous. In other words, when relations between stress, strain rate, and temperature are to be extracted from a Gleeble test, it is not always necessary to account for the inhomogeneities in the stress and strain rate fields.

1. INTRODUCTION

In order to understand, optimize and design the aluminium direct chill casting process, mathematical modelling is extensively used, addressing the heat and fluid flow, the microstructure development, and the thermally induced deformation and associated stress generation in the solidifying ingot. Important input to the latter class of models is a constitutive law relating the viscoplastic strain rate to the flow stress, temperature, and strain [1–6].

The coefficients in the constitutive equations are usually determined by tensile and/or compression testing, see e.g. References [7,8], or by creep tests, see e.g. References [6,9]. With conventional equipment for tensile testing, it is not straight forward to control the temperature. The Gleeble[1] machine provides possibilities to deal with this problem as well as handling the low strain rates (10^{-6} to $10^{-2}\,\mathrm{s}^{-1}$) characteristic for thermally induced deformations. By means of a Gleeble machine, Magnin *et al.* [5] determined the parameters of a modified Ludwig viscoplastic law for an Al-4.5%Cu alloy at temperatures between 50°C and 450°C and strain rates in the range 10^{-3} to $10^{-2}\,\mathrm{s}^{-1}$. In a similar way, Farup *et al.* [10] recently measured the flow stress at steady state creep in an AA3103 aluminium alloy. These tests were carried out at temperatures between 400 and 550 °C and for strain rates between 10^{-6} and $10^{-2}\ \mathrm{s}^{-1}$.

In the Gleeble machine, the specimen is heated by the Joule effect, and water cooled wedge jaws assure a high heat extraction at each side. Thus, only a small section at the centre is held at the prescribed temperature, and stress and strain rate are varying in the longitudinal direction of the specimen due to the temperature dependency of the flow stress. During the test, the temperature at the wedges increases slightly, and the associated thermal expansion is experimentally indistinguishable from elongation caused by viscoplastic deformation. Due to these phenomena, the global radial strain rate measured at the specimen centre by an extensometer was in References [5, 10] applied as the strain rate measure. The stress was set equal to the force in the axial direction divided by the current cross section area at the specimen centre. In order to make sure that the position of maximum straining really was at the specimen centre at which the controlling thermocouple was fixed, a slightly curved specimen geometry as indicated in Figure 1 was applied.

The application of such global strain rate and stress measures actually requires that the deformation is homogeneous and that the specimen is cylindrical. This was not fulfilled in the Gleeble tests in References [5, 10]. In order to investigate the inaccuracy associated with using the global radial strain rate

[1] Gleeble is a registered trademark of Dynamic Systems Inc.

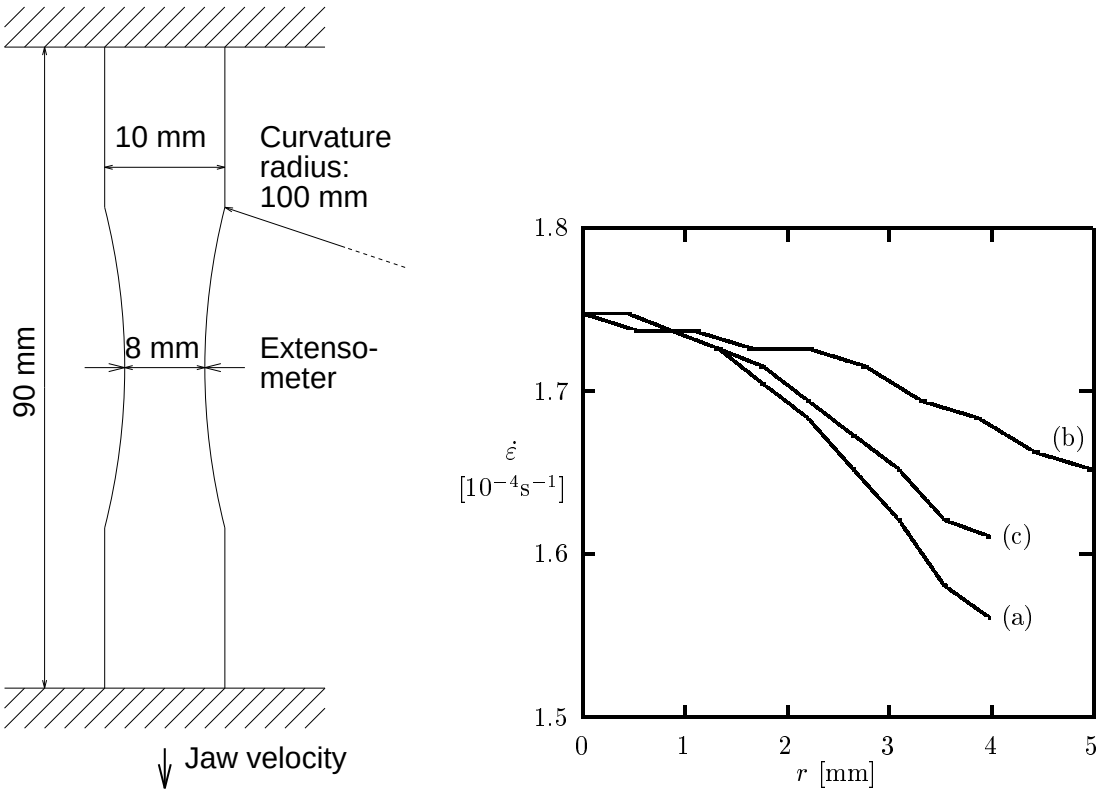

Figure 1: Left: Gleeble test specimen in the experiments in Reference [10] and in the finite element model. Right: ABAQUS calculated effective viscoplastic strain rate, $\dot{\varepsilon}$, *versus* radial distance from the specimen centre, r, during steady state in three cases, all with $475\ ^\circ$C and a viscoplastic strain rate of $1.75 \times 10^{-4}\ \mathrm{s}^{-1}$ at the specimen centre. Graph (a): same specimen and temperature distribution as in the experiments. Graph (b): cylindrical specimen (diameter 10 mm) with the same temperature distribution as in the experiments. Graph (c): specimen with a homogeneous temperature (same geometry as in the experiments).

and the axial force divided by the cross section area at the specimen centre as measures for the strain rate and stress when coefficients in constitutive equations are to be determined, experiments similar to those in Reference [10] are in the present paper simulated by ABAQUS.[2]

2. GLEEBLE TEST RESULTS

The effective viscoplastic strain rate was in References [5, 10] defined by

$$\dot{\varepsilon}_{homo} = -2\left[\frac{1}{r}\frac{dr}{dt} + \frac{\nu}{E}\frac{d}{dt}\left(\frac{F}{A}\right)\right] \tag{1}$$

where t, r, F, A, E, and ν denote time, current radius, axial force, current cross section area, Young's modulus, and Poisson's ratio, respectively. The quantity F/A was furthermore applied as measure for the stress. These definitions actually correspond to what would be the situation if the specimen were cylindrical and the temperature, stress, and strain rate fields were homogeneous.

In Reference [10], $\dot{\varepsilon}_{homo}$ was set equal to the slope of the global strain *versus* time in the period during which this curve is approximately linear. The resulting experimental points are displayed in Figure 2 along with the creep law in which the coefficients are determined by minimizing the squared error in $\log(\dot{\varepsilon}_{homo})$ by means of the simulated annealing technique [11].

3. FINITE ELEMENT MODEL

The specimen geometry in the ABAQUS model is similar to that in the Gleeble testing in Reference [10] and shown in Figure 1. The free part of the specimen is considered as the solution domain (which is reduced to a quarter due to the axial symmetry). This is subjected to a pre-defined axial velocity by the jaws. The material is considered as viscoelastic, and the relation between stress, viscoplastic strain rate, and temperature at steady state creep is given by the solid curve in Figure 2. Coefficients for Hookes' law are taken from Reference [12, pages 81–83]. Quadrilateral, bilinear, axisymmetric elements are used, and

[2] ABAQUS is a general purpose finite element code from Hibbit, Karlsson & Sorensen Inc., Pawtucket, RI, USA.

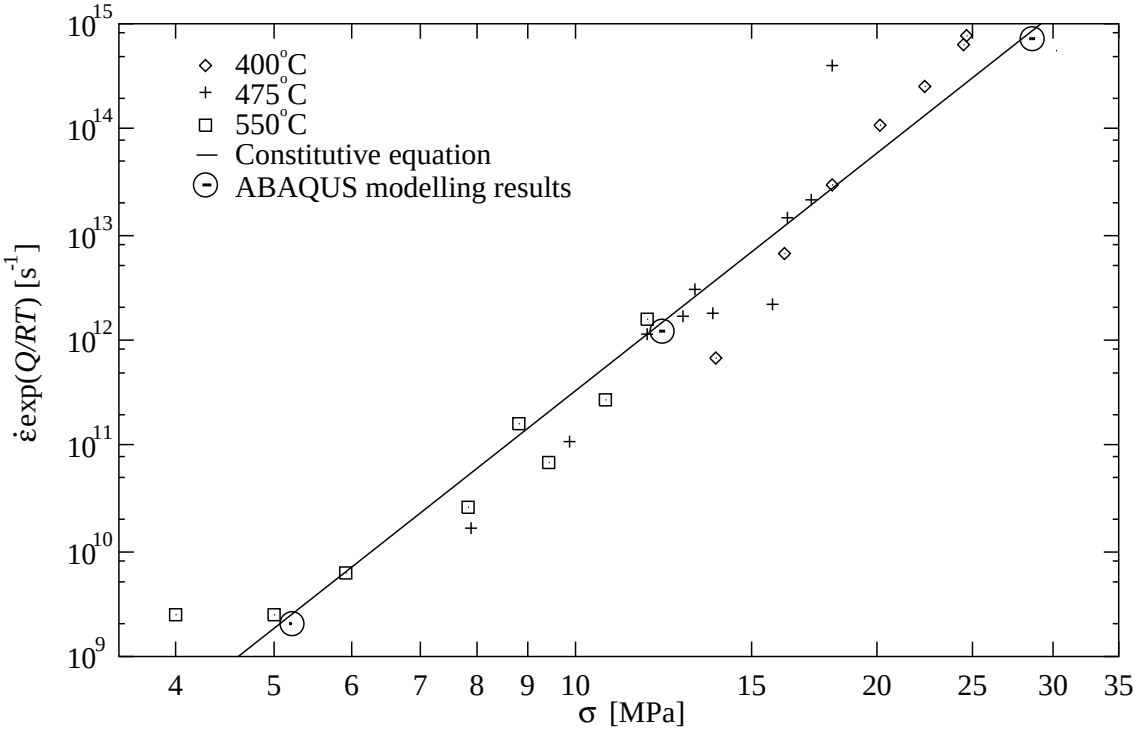

Figure 2: Gleeble test results for an AA3103 alloy during steady state creep [10] for which $\dot{\varepsilon}_{homo}$ and F/A (defined in the text) are interpreted as the effective viscoplastic strain rate, $\dot{\varepsilon}$, and stress, σ, respectively. The solid curve is the creep law $\dot{\varepsilon}\exp(Q/RT) = A[\sinh(\sigma/\sigma_0)]^n$ in which T denotes temperature and the coefficients are determined by the simulated annealing technique [11]: $Q/R = 27300$ K, $A = 1.55 \times 10^{25}$ s^{-1}, $\sigma_0 = 670$ MPa, and $n = 7.5$. The small line segments (within circles) represent ABAQUS calculations of $\dot{\varepsilon}_{homo}$ and F/A during steady state creep.

because the specimen geometry is smooth and the temperature varies smoothly over the specimen, 310 nodes have been found to give sufficient accuracy.

The temperature profile in the longitudinal direction is considered as known input to the model. It is a good approximation to the experimental situation to assume a parabolic profile with maximum at the specimen centre being about 175 K higher than at the jaws. Three cases with different temperatures and strain rates are modelled. The jaw velocity and temperatures in the specimen centre and at the surface in contact with the jaw are given in Table 1 for these three cases.

Table 1: ABAQUS case studies.

Jaw velocity $[10^{-6}\text{ms}^{-1}]$	Temperature centre [°C]	Temperature jaw surface [°C]
0.05	550	375
1	475	300
10	400	225

4. MODELLING RESULTS

The inhomogeneities in the strain rate field induced by the axial temperature profile and by the curved geometry are quantified in Figure 1. In Graph (a), it is seen that the effective viscoplastic strain rate varies between 1.75×10^{-4} s^{-1} at the centre to 1.56×10^{-4} s^{-1} at the surface, i.e., by about 10 %. Graph (b) reveals the inhomogenity in $\dot{\varepsilon}$ induced by the axial temperature gradient when the specimen is a cylinder, while Graph (c) quantifies the inhomogeneity induced by the curved geometry alone (homogeneous temperature). It is seen that the temperature variation along the specimen and the curving both contribute to the inhomogeneity.

Steady state conditions similar to those in the experiments develop in the ABAQUS modelling (although the transient phase is different from the experimental situation due to the neglect of work harding in the constitutive equations). For the three cases defined in Table 1, calculated steady state values for $\dot{\varepsilon}_{homo}$ and F/A are displayed in Figure 2 as three small line segments (within circles). The time periods associated with these line segments correspond to the steady state regime in the experiments. In other words, they are similar to the periods of linearity in the strain *versus* time curves measured by the Gleeble machine during which the measured points in Figure 2 were extracted. It is seen that the discrepancy between the line segments and the solid curve representing the constitutive law (being input to the ABAQUS modelling) is quite small, and definitely smaller than the average distance between the solid curve and the experimental points. The error associated with the curve fitting is in other words larger than the error associated with applying $\dot{\varepsilon}_{homo}$ and F/A as measures for strain rate and stress, respectively.

5. CONCLUSION

Inhomogeneities in the stress and strain rate fields during Gleeble testing of steady state creep at temperatures between 400 and 550 °C and strain rates between 10^{-6} and 10^{-2} s^{-1} have been studied by finite element modelling. Axisymmetric test specimens with length 90 mm have been modelled, and the diameter varies between 8 mm at the centre and 10 mm at the jaws. The temperature variation along the specimen is parabolic with a maximum at the centre 175 K larger than at the jaws. The calculations show that the relative differences in effective viscoplastic strain rate along the radius at the specimen centre is about 10 %. It is furthermore showed that when constitutive relations are to be extracted from Gleeble tests, the error associated with curve fitting is often larger than the error associated with applying the global radial strain rate and the axial force divided by the cross section area at the specimen centre as measures of strain rate and stress, respectively, i.e., assuming homogeneous deformation in the test specimen.

Acknowledgement

Funding from Elkem Aluminium, Hydro Aluminium, Hydro Raufoss Automotive Research center, and the Research Council of Norway through the project *PROSMAT-Støperikompetanse* is greatly acknowledged.

REFERENCES

[1] V. M. Sample and L. A. Lalli. *Materials Science and Technology*, **3**:28–35, 1987.

[2] R. E. Smelser and O. Richmond. In A. F. Giamei and G. J. Abbaschian, editors, *Modeling and Control of Casting and Welding Processes IV*, pages 313–328. TMS-AIME, 1988.

[3] H. D. Brody, P. Wisniewskih, A. G. Gokhale, and J. Mathew. In A. F. Giamei and G. J. Abbaschian, editors, *Modeling and Control of Casting and Welding Processes IV*, pages 351–360. TMS-AIME, 1988.

[4] H. G. Fjær and A. Mo. *Metallurgical Transactions*, **21B**:1049–1061, 1990.

[5] B. Magnin, L. Katgerman, and B. Hannart. In M. Cross and J. Campbell, editors, *Modelling of casting, welding and advanced solidification processes—VII*, pages 303–310. TMS-AIME, 1995.

[6] J.-M. Drezet and M. Rappaz. *Metallurgical and Materials Transactions*, **27A**:3214–3225, 1996.

[7] M. L. Nedreberg. *Thermal stress and the hot tearing during the DC casting of AlMgSi billets.* PhD thesis, University of Oslo, Dep. of Physics, February 1991.

[8] P. Wisniewski and H. D. Brody. In M. Rappaz, M. R. Özgü, and K. W. Mahin, editors, *Modeling and control of casting and welding processes V*, pages 273–278. TMS-AIME, 1991.

[9] J.-M. Drezet and G. Eggeler. *Scripta Metallurgica*, **31**(6):757–762, 1994.

[10] I. Farup, J.-M. Drezet, A. Mo, and T. Iveland. To be submitted to the *Journal of Applied Mechanics*, 1998.

[11] S. Kirkpatrick, C. D. Gelatt, and M. P. Vecchi. *Science*, **220**(4598):671–680, 1983.

[12] L. F. Mondolfo. *ALUMINIUM ALLOYS: Structure and properties*. Butter Worths, 1976.